European Journal of Mechanics B/Fluids 28 (2009) 117–126

Contents lists available at ScienceDirect

European Journal of Mechanics B/Fluids

www.elsevier.com/locate/ejmflu

Criticality manifolds and their role in the generation of solitary waves for two-layer flow with a free surface

Thomas J. Bridges *, Neil M. Donaldson

Department of Mathematics, University of Surrey, Guildford, Surrey, GU2 7XH, England

ARTICLE INFO

Article history:
Received 19 October 2007
Received in revised form 2 May 2008
Accepted 2 May 2008
Available online 24 May 2008

Keywords:
Stratified flow
Free surface
Solitary waves
Differential geometry of surfaces

ABSTRACT

The role of criticality manifolds is explored both for the classification of all uniform flows and for the bifurcation of solitary waves, in the context of two fluid layers of differing density with an upper free surface. While the weakly nonlinear bifurcation of solitary waves in this context is well known, it is shown herein that the critical nonlinear behaviour of the bifurcating solitary waves and generalized solitary waves is determined by the geometry of the criticality manifolds. By parametrizing all uniform flows, new physical results are obtained on the implication of a velocity difference between the two layers on the bifurcating solitary waves.

© 2008 Elsevier Masson SAS. All rights reserved.

1. Introduction

The inviscid flow of two layers of homogeneous fluid of differing density with a free surface above the second layer is a useful simplified model for stratified flow in the atmosphere and ocean. Criticality of the uniform flows provides an organizing center for the bifurcation of internal fronts and solitary waves (see recent reviews of Grimshaw [14] and Helfrich and Melville [15] and references therein). In this paper the theory of criticality manifolds is applied to the two layer system with an upper free surface.

Our main results are (a) the four-parameter family of uniform flows can be parametrized by the criticality surfaces in the 5-dimensional space associated with the total momentum flux and the two mass fluxes and two Bernoulli energies, highlighting the criticality submanifolds. (b) The nonlinear coefficient needed for the bifurcation of solitary waves is determined by second derivatives of the criticality mapping. (c) Previous results on bifurcating solitary waves are extended to the case where there is a velocity difference between the lower and upper layer.

Before proceeding further it will be useful to define exactly what we mean by "criticality manifolds". Effectively this is a new interpretation of information that is fundamental in hydraulics. The shallow water equations for two layers with a free surface take the following familiar form (cf. §3.3 of Baines [3])

$$\begin{aligned}
&\frac{\partial}{\partial t}(\rho_1 h_1) + \frac{\partial}{\partial x}(\rho_1 h_1 u_1) = 0,\\
&\frac{\partial}{\partial t}(\rho_2 h_2) + \frac{\partial}{\partial x}(\rho_2 h_2 u_2) = 0,\\
&\frac{\partial}{\partial t}(\rho_1 u_1) + \frac{\partial}{\partial x}\left(\frac{1}{2}\rho_1 u_1^2 + \rho_1 g h_1 + \rho_2 g h_2\right) = 0,\\
&\frac{\partial}{\partial t}(\rho_2 u_2) + \frac{\partial}{\partial x}\left(\frac{1}{2}\rho_2 u_2^2 + \rho_2 g h_1 + \rho_2 g h_2\right) = 0.
\end{aligned} \tag{1.1}$$

In these equations $u_1(x,t)$ and $u_2(x,t)$ are the depth-averaged horizontal velocities, $h_1(x,t)$ and $h_2(x,t)$ are the layer depths, g is the gravitational constant and ρ_1 and ρ_2 are the fluid density in each layer, with 1 associated with the lower layer and 2 associated with the upper layer. It is shown by Barros [4] that these equations can be written in the illuminating form

$$\mathbf{c}_t + \big(\mathbf{M}\nabla E(\mathbf{c})\big)_x = 0,$$

by taking $\mathbf{c} = (h_1, h_2, u_1, u_2)$,

$$\mathbf{M} = \begin{bmatrix} 0 & 0 & \frac{1}{\rho_1} & 0\\ 0 & 0 & 0 & \frac{1}{\rho_2}\\ \frac{1}{\rho_1} & 0 & 0 & 0\\ 0 & \frac{1}{\rho_2} & 0 & 0 \end{bmatrix}$$

and

$$E(\mathbf{c}) = \frac{1}{2}\rho_1 h_1 u_1^2 + \frac{1}{2}\rho_2 h_2 u_2^2 + \frac{1}{2}\rho_1 g h_1^2 + \rho_2 g h_1 h_2 + \frac{1}{2}\rho_2 g h_2^2. \tag{1.2}$$

The function $E(\mathbf{c})$ corresponds to the energy of the system.

Steady flows – which in this case are uniform flows – satisfy these equations with the time-derivative terms dropped. Uniform

* Corresponding author.
E-mail address: t.bridges@surrey.ac.uk (T.J. Bridges).

0997-7546/$ – see front matter © 2008 Elsevier Masson SAS. All rights reserved.
doi:10.1016/j.euromechflu.2008.05.003

flows therefore correspond to constant values of (R_1, R_2, Q_1, Q_2) with

$$R_1 := \frac{\partial E}{\partial h_1} = \frac{1}{2}\rho_1 u_1^2 + \rho_1 g h_1 + \rho_2 g h_2,$$
$$R_2 := \frac{\partial E}{\partial h_2} = \frac{1}{2}\rho_2 u_2^2 + \rho_2 g h_1 + \rho_2 g h_2,$$
$$Q_1 := \frac{\partial E}{\partial u_1} = \rho_1 h_1 u_1,$$
$$Q_2 := \frac{\partial E}{\partial u_2} = \rho_2 h_2 u_2. \tag{1.3}$$

These expressions are just the Bernoulli energy (R_1 and R_2) and mass flux (Q_1 and Q_2) in each layer. With $\mathbf{P} = (R_1, R_2, Q_1, Q_2)$, (1.3) is the mapping $\mathbf{P}:\mathbb{R}^4 \to \mathbb{R}^4$. It is remarkable how much information this simple mapping contains.

First, the mapping $\mathbf{P}(\mathbf{c})$ parametrizes all uniform flows. This parametrization is explored in Section 2. Secondly a uniform flow is critical if $\det[\mathrm{D}\mathbf{P}(\mathbf{c})] = 0$ where

$$\mathrm{D}\mathbf{P}(\mathbf{c}) := \begin{bmatrix} \frac{\partial R_1}{\partial h_1} & \frac{\partial R_1}{\partial h_2} & \frac{\partial R_1}{\partial u_1} & \frac{\partial R_1}{\partial u_2} \\ \frac{\partial R_2}{\partial h_1} & \frac{\partial R_2}{\partial h_2} & \frac{\partial R_2}{\partial u_1} & \frac{\partial R_2}{\partial u_2} \\ \frac{\partial Q_1}{\partial h_1} & \frac{\partial Q_1}{\partial h_2} & \frac{\partial Q_1}{\partial u_1} & \frac{\partial Q_1}{\partial u_2} \\ \frac{\partial Q_2}{\partial h_1} & \frac{\partial Q_2}{\partial h_2} & \frac{\partial Q_2}{\partial u_1} & \frac{\partial Q_2}{\partial u_2} \end{bmatrix}.$$

Indeed, a straightforward calculation shows that

$$\begin{aligned}\det\big(\mathrm{D}\mathbf{P}(\mathbf{c})\big) &= \rho_1^2\rho_2^2\big[u_1^2u_2^2 - gh_2u_1^2 - gh_1u_2^2 + (1-r)g^2h_1h_2\big] \\ &= \rho_1^2\rho_2^2(1-r)gh_1gh_2\big[1 - F_1^2 - F_2^2 + (1-r)F_1^2F_2^2\big],\end{aligned} \tag{1.4}$$

where

$$F_j^2 = \frac{u_j^2}{g(1-r)h_j}, \quad r = \frac{\rho_2}{\rho_1}.$$

Setting $\det(\mathrm{D}\mathbf{P}(\mathbf{c})) = 0$ recovers the familiar condition for criticality of two-layer flow with a free surface (cf. Armi [1], Baines [3] and references therein). However, there is a great deal more information available here. Criticality $\det(\mathrm{D}\mathbf{P}(\mathbf{c})) = 0$ defines a three-dimensional hypersurface in the four-dimensional $\mathbf{c}$-space. The geometry of this hypersurface is explored in Section 3. The fact that $\mathrm{D}\mathbf{P}(\mathbf{c})$ is singular assures the existence of an eigenvector $\mathbf{n} \in \mathbb{R}^4$ satisfying

$$\mathrm{D}\mathbf{P}(\mathbf{c})\mathbf{n} = 0.$$

This eigenvector provides geometric information about the criticality surface. The third observation is that the second derivative of $\mathbf{P}$ in the direction $\mathbf{n}$ gives information about solitary waves and generalized solitary waves. The precise form of the second derivative is

$$\begin{aligned}\frac{d^2}{ds^2}\big(\mathbf{n}^T\mathbf{P}(\mathbf{c}+s\mathbf{n})\big)\bigg|_{s=0} &= \mathsf{C}(\mathbf{c})\big(m^2\ell^2r^2 + m\ell(3m - 3\ell - 1)r \\ &\quad + (m-\ell)^3\big),\end{aligned} \tag{1.5}$$

where $\mathbf{c}$ satisfies (1.4), $\mathsf{C}(\mathbf{c})$ is a nonzero function and

$$m := \frac{h_2}{h_1}, \qquad \ell := \frac{u_2^2}{u_1^2}. \tag{1.6}$$

The remarkable feature of the right-hand side of (1.5) is that it is the critical coefficient needed for the bifurcation of solitary waves. When $\ell = 1$ this expression reduces to a multiple of α_- in Eq. (3.8) of Kakutani and Yamasaki [16] and a multiple of Λ in Eq. (3.5) in Dias and Il'ichev [12] (see also Peters and Stoker [19] – who first pointed out the existence of this singularity – and Walker [21]). The precise relation between the right-hand side of (1.5) and the results in [16] and [12] is discussed in Sections 4.1 and 4.2. By allowing the ratio of the velocities ℓ to vary, new properties of the zero set of the right-hand side of (1.5) appear.

The bifurcation of solitary waves and generalized solitary waves for this fluid configuration is well known, even to finite amplitude (cf. Dias and Il'ichev [12], Michallet and Dias [18], Barros and Gavrilyuk [5] and references therein). Our new observations about bifurcating solitary waves are twofold: to show the role of the mapping $\mathbf{P}(\mathbf{c})$ in the bifurcation of solitary waves, and to extend the range of parameter space by including a velocity difference between the two layers.

Our starting point for the weakly nonlinear bifurcation of solitary waves and generalized solitary waves is the normal form of Dias and Il'ichev [12]. They show that the leading order normal form for bifurcating solitary waves near the slow critical curve (this curve is defined in Fig. 7) takes the form

$$\begin{aligned}-\frac{dv}{dx} &= I_1 - \frac{1}{2}\kappa u^2 + \nu|A|^2 + \cdots, \\ \frac{du}{dx} &= s_1 v + \cdots, \\ \frac{dA}{dx} &= \mathrm{i}\omega A + \mathrm{i}\nu u A + \cdots\end{aligned} \tag{1.7}$$

where u, v are real-valued functions, $A(x)$ is a complex-valued function, i is the imaginary unit, $s_1 = \pm 1$ and κ, ν, ω and I_1 are real parameters. This normal form is given in Eq. (3.15) of [12]. It has been adjusted in this case to reflect the Hamiltonian structure. The properties of this normal form are discussed in Section 6.1. The coefficient κ is called Λ in [12], and it is the critical coefficient associated with bifurcation of solitary waves. One of our principal observations is the connection between κ and the mapping $\mathbf{P}(\mathbf{c})$,

$$\kappa = a_1^3\frac{d^2}{ds^2}\big(\mathbf{n}^T\mathbf{P}(\mathbf{c}+s\mathbf{n})\big)\bigg|_{s=0}, \tag{1.8}$$

where a_1 is just a positive scale factor. This observation is a special case of the theory of normal forms for degenerate relative equilibria [7–10], and is discussed in Section 6.1.

The solitary waves predicted by the normal form (1.7) are generalized solitary waves; that is, they do not in general decay to zero as $x \to \pm\infty$. Their tails can be exponentially small. This issue has been well-studied in the literature (see Lombardi [17] and Dias and Il'ichev [12] and references therein) and will not be considered here. Here, only the geometric properties of the leading order normal form are discussed.

2. Uniform flows in (Q_1, Q_2, S) space

In this section it is shown how the mapping (1.3) parametrizes uniform flows. To see the basic strategy, first consider the case of one fluid layer. For one layer, (1.3) reduces to

$$R = gh + \frac{1}{2}u^2, \qquad Q = hu, \tag{2.1}$$

where $g > 0$ is the gravitational constant. Accompanying these two functions is the momentum flux

$$S = hu^2 + \frac{1}{2}gh^2.$$

For given values of R and Q, uniform flows correspond to solutions of (2.1) when the mapping from (R, Q) to (h, u) is uniquely invertible. The singular points can be included by lifting the family of uniform flows into the three-dimensional (R, Q, S) space by including the momentum flux. Uniform flows in this 3D space lie

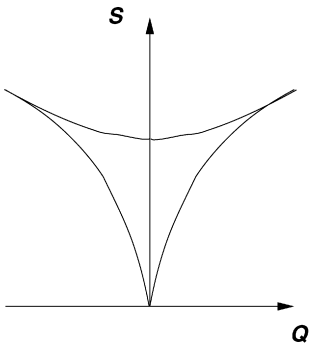

Fig. 1. Slice with constant $R > 0$ of the surface of uniform flows in the (R, Q, S) space.

on a swallowtail, and a cut through the swallowtail for $R > 0$ is shown in Fig. 1. The two cusp points on the surface correspond to critical flow. This approach to the plotting of uniform flows in the SQR space is due to Sewell and Porter [20].

This figure shows that one cannot choose uniform flows arbitrarily. Every possible uniform flow, for each fixed $R > 0$, lies on a single curve in (S, Q) space, and there are exactly two points (the cusps) where the uniform flow is critical and they correspond to $F = \pm 1$ where R is the usual Froude number.

This approach to parametrization of uniform flows is now generalized to two-layer flow with a free surface. Accompanying the functions (R_1, R_2, Q_1, Q_2) is the momentum flux

$$\begin{aligned} S &= \langle \mathbf{c}, \nabla E(\mathbf{c}) \rangle - E(\mathbf{c}) \\ &= h_1 R_1 + h_2 R_2 + u_1 Q_1 + u_2 Q_2 - E \\ &= \rho_1 h_1 u_1^2 + \rho_2 h_2 u_2^2 + \frac{1}{2}\rho_1 g h_1^2 + \rho_2 g h_1 h_2 + \frac{1}{2}\rho_2 g h_2^2, \end{aligned} \tag{2.2}$$

which is obtained from the shallow-water equations (1.1) by noting that

$$\frac{\partial I}{\partial t} + \frac{\partial S}{\partial x} = 0,$$

with

$$I = \frac{1}{2}\langle \mathbf{M}^{-1}\mathbf{c}, \mathbf{c} \rangle = \rho_1 h_1 u_1 + \rho_2 h_2 u_2.$$

See Barros [4] for further discussion of the conservation laws for two-layer flow with a free surface.

The functions in (1.3) and (2.2) can be viewed as a mapping from $\mathbb{R}^4 = \{(h_1, h_2, u_1, u_2)\colon\ h_1 > 0,\ h_2 > 0\}$ to $\mathbb{R}^5 = \{S, Q_1, Q_2, R_1, R_2\}$. This surface is a generalization of the swallowtail in the case of a single layer fluid shown in Fig. 1.

Taking R_1 and R_2 fixed, h_1 and h_2 can be expressed as functions of r, R_1, R_2 and the velocities

$$\begin{aligned} h_1 &= \frac{1}{\rho_1 g(1-r)}\left(R_1 - R_2 - \frac{1}{2}\rho_1 u_1^2 + \frac{1}{2}\rho_2 u_2^2\right), \\ h_2 &= \frac{1}{\rho_1 g r(1-r)}\left(-rR_1 + R_2 + \frac{1}{2}\rho_2 u_1^2 - \frac{1}{2}\rho_2 u_2^2\right). \end{aligned} \tag{2.3}$$

The regions of feasible uniform flows in the velocity space (u_1^2, u_2^2) are determined by the physical requirement that $h_1 > 0$ and $h_2 > 0$. These conditions provide lines which border the region of feasible uniform flows

$$\begin{aligned} &\frac{2}{\rho_1}(R_1 - R_2) \geqslant u_1^2 - r u_2^2, \\ &\frac{2}{\rho_2}(R_2 - rR_1) \geqslant -u_1^2 + u_2^2. \end{aligned} \tag{2.4}$$

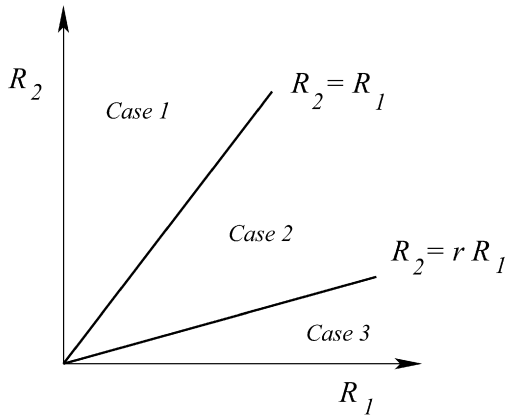

Fig. 2. Regions corresponding to Cases 1, 2 and 3 in the Bernoulli energy space.

Fortunately the intersection of these two sets is finite. In fact setting $h_1 = h_2 = 0$ shows that there is a strict upper bound on admissible velocity fields

$$u_1^2 \leqslant \frac{2}{\rho_1}R_1, \qquad u_2^2 \leqslant \frac{2}{\rho_2}R_2.$$

This bound is to be contrasted with the case of two layers with a rigid lid [10] where the field of admissible velocities is infinite – even when R_1 and R_2 are finite.

There are three cases depending on the values of R_1 and R_2:

Case 1: $R_2 > R_1$, Case 2: $rR_1 < R_2 < R_1$, Case 3: $R_2 < rR_1$.

These three cases divide the positive quadrant of the Bernoulli energy space (R_1, R_2) into three regions as shown in Fig. 2. For each subregion in the Bernoulli energy space, the feasible regions in velocity space need to be determined and they are shown in Fig. 3. In Case 1 the upper layer is dominant; in Case 3 the lower layer is dominant and in Case 2 the two layers are in balance. Case 2 is the most interesting as there are two regions of critical flow (see Fig. 7 below). Substituting the expressions for h_1 and h_2 into Q_1, Q_2 and S with fixed r, R_1 and R_2 results in a parameterized hypersurface in the three-dimensional (Q_1, Q_2, S) space,

$$\begin{aligned} Q_1(u_1, u_2) &= \frac{\rho_1}{2g(1-r)}u_1\left(2\frac{R_1}{\rho_1} - 2\frac{R_2}{\rho_1} - u_1^2 + ru_2^2\right), \\ Q_2(u_1, u_2) &= \frac{\rho_2}{2g(1-r)}u_2\left(-2\frac{R_1}{\rho_1} + 2\frac{R_2}{\rho_2} + u_1^2 - u_2^2\right) \end{aligned}$$

with a similar expression for $S(u_1, u_2)$ obtained by substituting (2.3) into S in (2.2). By letting (u_1, u_2) vary over the feasible region, curves in the (Q_1, Q_2, S) space are generated and examples of the three cases are shown in Figs. 4–6.

In these figures the curves of critical uniform flows are colored in red. These figures are best viewed interactively in MAPLE where they can be rotated and enlarged, and copies of the MAPLE codes which generated these figures are available for downloading.[1]

2.1. Criticality hyperbolae in velocity and Froude number space

In Figs. 4–6 the subsets of uniform flows corresponding to critical flow are colored in red. In black and white, the lines of criticality are the thicker lines in the interior of the triangular regions. These are the subsets which satisfy the criticality condition (1.4). The criticality curves in (Q_1, Q_2, S) space are the image of the criticality curves in the velocity space. The criticality curves in velocity

[1] http://personal.maths.surrey.ac.uk/st/T.Bridges/TWO-LAYER/.

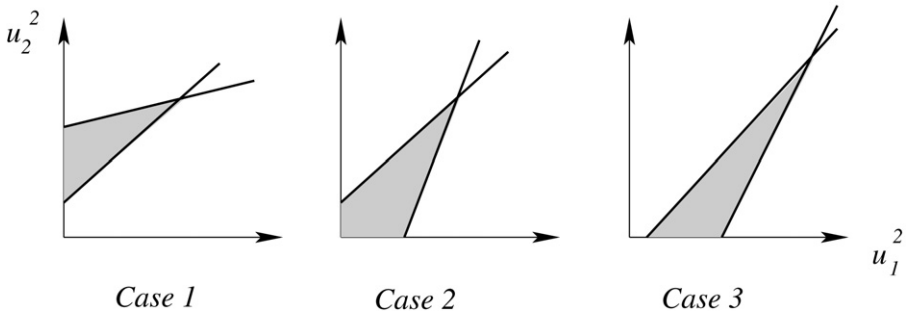

Fig. 3. Schematic of feasible regions of uniform flows in velocity space. The shaded regions consist of admissible velocity fields for uniform flow. Equations for the upper and lower boundaries are given in (2.4).

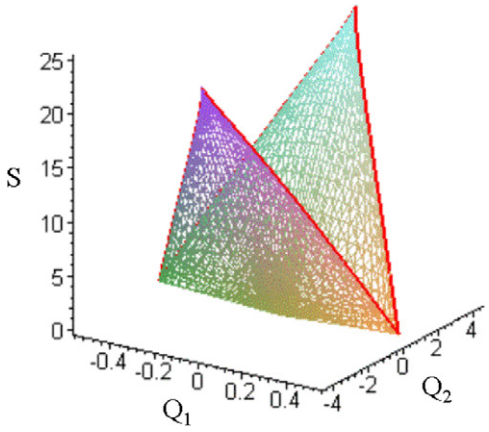

(a) The surface of uniform flows associated with Case 1.

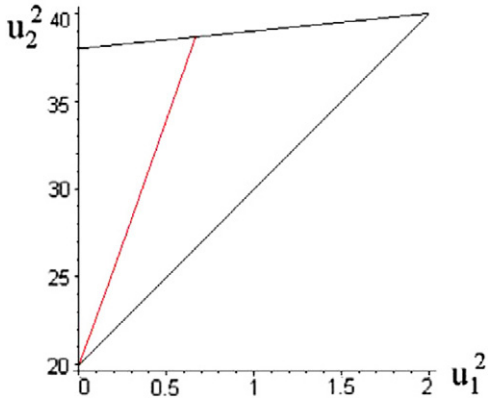

(b) The criticality hyperbola in velocity space superimposed on the region of uniform flows.

Fig. 4. Surface of uniform flows and criticality curves corresponding to Case 1, in terms of scaled variables with $\rho_1 = 1$, $g = 1$, $r = 0.1$ and $R_1 = 1$ and $R_2 = 2$.

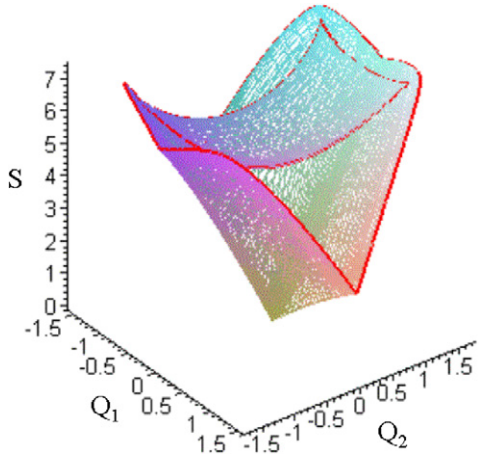

(a) The surface of uniform flows associated with Case 2.

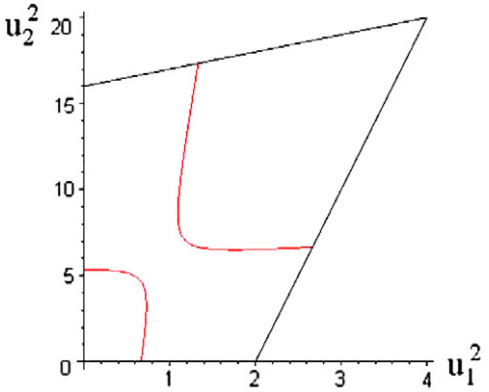

(b) The criticality hyperbola in velocity space superimposed on the region of uniform flows.

Fig. 5. Surface of uniform flows and criticality curves corresponding to Case 2, in terms of scaled variables with $\rho_1 = 1$, $g = 1$, $r = 0.1$ and $R_1 = 2$ and $R_2 = 1$.

space are determined as follows. Substitute (2.3) into the criticality condition (1.4). This gives a conic section in u_1^2 and u_2^2 which turns out to be hyperbolae in all three cases (see §3.4.2 of [13]). The intersection of these hyperbolae with the admissible regions in velocity space are shown in Figs. 4(b), 5(b) and 6(b). The most interesting case is Case 2 where both branches of the hyperbola appear.

Another way to view the fast and slow critical curves is in the Froude number plane. The criticality condition (1.4) can be expressed in the form

$$\big[(1-r)F_1^2 - 1\big]\big[(1-r)F_2^2 - 1\big] = r, \tag{2.5}$$

from which the following parameterization is immediate,

$$F_1^2 = \frac{1 \pm \sqrt{r}\,\mathrm{e}^{+\varphi}}{1-r} \quad \text{and} \quad F_2^2 = \frac{1 \pm \sqrt{r}\,\mathrm{e}^{-\varphi}}{1-r},$$

and these curves are shown in Fig. 7. The plus sign is for the fast critical mode and the minus sign is for the slow critical mode. For the fast critical mode, $-\infty < \varphi < +\infty$, but for the slow mode φ is restricted by $\sqrt{r} \leqslant \mathrm{e}^{\varphi} \leqslant \frac{1}{\sqrt{r}}$.

3. Geometry of the criticality surfaces in (R, Q) space

The curves in the (Q_1, Q_2, S) space with (R_1, R_2) fixed show all uniform flows, and the critical flows arise as cusp curves on these surfaces. As (R_1, R_2) vary these criticality curves become 3-dimensional criticality surfaces. In this section the properties of

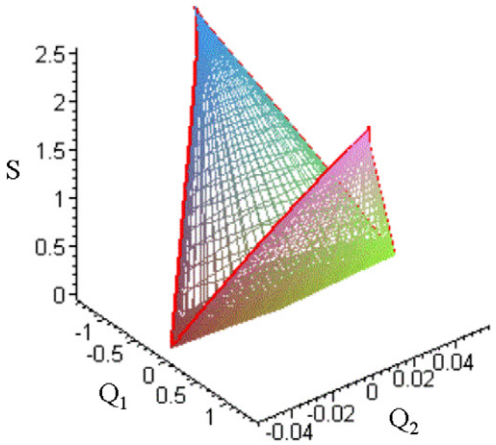

(a) The surface of uniform flows associated with Case 3.

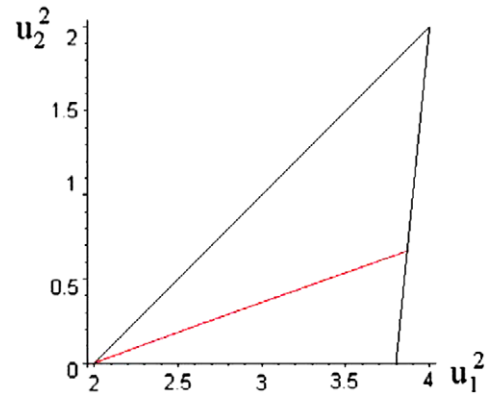

(b) The criticality hyperbola in velocity space superimposed on the region of uniform flows.

Fig. 6. Surface of uniform flows and criticality curves corresponding to Case 3, in terms of scaled variables with $\rho_1 = 1$, $g = 1$, $r = 0.1$ and $R_1 = 2$ and $R_2 = 0.1$.

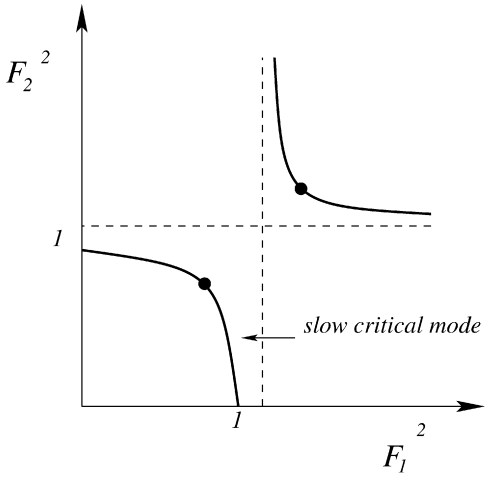

Fig. 7. Schematic of the criticality curves in the Froude number plane. The dashed lines correspond to the asymptotes: $F_1^2 = (1-r)^{-1}$ and $F_2^2 = (1-r)^{-1}$. The dots correspond to the points on the two criticality curves where $F_1^2 = F_2^2$ and their coordinates are $(1 \pm \sqrt{r})^{-1}$.

these criticality surfaces are explored, based on an analysis of the mapping $\mathbf{P}(\mathbf{c})$ introduced in Section 1.

The study of $\mathbf{P}(\mathbf{c})$ is also related to the relative equilibrium characterization of uniform flows and this theory is given in Chapter 4 of Donaldson [13]. The upshot of that analysis is that uniform flows are critical precisely when the Jacobian of the mapping $\mathbf{P}(\mathbf{c})$ is degenerate, $\det[\mathrm{D}\mathbf{P}(\mathbf{c})] = 0$. The Jacobian is given explicitly by

$$\mathrm{D}\mathbf{P}(\mathbf{c}) = \begin{bmatrix} \rho_1 g & \rho_2 g & \rho_1 u_1 & 0 \\ \rho_2 g & \rho_2 g & 0 & \rho_2 u_2 \\ \rho_1 u_1 & 0 & \rho_1 h_1 & 0 \\ 0 & \rho_2 u_2 & 0 & \rho_2 h_2 \end{bmatrix}. \tag{3.1}$$

Note that the Jacobian is a symmetric matrix. The symmetry follows from (1.3) which shows that $\mathbf{P}(\mathbf{c}) = \nabla E(\mathbf{c})$. Setting the determinant of $\mathrm{D}\mathbf{P}(\mathbf{c})$ to zero gives the criticality condition for two-layer uniform flows with a free surface as noted in (1.4).

The simplest version of criticality is when the Jacobian $\mathrm{D}\mathbf{P}(\mathbf{c})$ has a simple eigenvalue; that is, the Jacobian has rank 3. The matrix $\mathrm{D}\mathbf{P}(\mathbf{c})$ has rank three if

$$\Delta'(0) \neq 0 \quad \text{where } \Delta(\lambda) = \det\big[\mathrm{D}\mathbf{P}(\mathbf{c}) - \lambda \mathbf{I}\big],$$
$$\text{when } \Delta(0) = \det\big(\mathrm{D}\mathbf{P}(\mathbf{c})\big) = 0.$$

Expanding out the determinant and differentiating

$$\begin{aligned}\Delta'(0) = r\rho_1^3\big[&-g^2h_1 - rg^2h_2 - gh_1h_2 + rgu_2^2 - gh_1rh_2 \\ &+ ru_2^2h_1 + g^2rh_1 + g^2r^2h_2 + u_1^2g + u_1^2h_2\big].\end{aligned} \tag{3.2}$$

The right-hand side should be evaluated for $\mathbf{c}$ satisfying the criticality condition (1.4). It is proved in Appendix A that $\Delta'(0)$ is nonzero for all physically admissible values of the parameters. Hence, zero is a simple eigenvalue of $\mathrm{D}\mathbf{P}(\mathbf{c})$ with eigenvector

$$\mathrm{D}\mathbf{P}(\mathbf{c})\mathbf{n} = 0 \quad \Rightarrow \quad \mathbf{n} = \mathbb{R}\begin{pmatrix} rgh_1h_2 \\ h_2(u_1^2 - gh_1) \\ -rgh_2u_1 \\ -u_2(u_1^2 - gh_1) \end{pmatrix}, \tag{3.3}$$

where $\mathbb{R}$ represents an arbitrary multiplicative constant. Since it does not affect the later discussion, take the multiplicative constant to be unity. The symbol $\mathbf{n}$ is used since $\mathbf{n}$ can be interpreted as a normal vector – *to the image of the criticality surface in* (R_1, R_2, Q_1, Q_2) *space* (cf. Fig. 9 of [9]).

The condition $\det[\mathrm{D}\mathbf{P}(\mathbf{c})] = 0$ defines a 3-dimensional hypersurface in the 4-dimensional $\mathbf{c}$-space, and this surface can be parametrized by taking

$$\begin{aligned} h_1(s,t,\varphi) &= s, \\ h_2(s,t,\varphi) &= t, \\ u_1(s,t,\varphi) &= \pm\sqrt{gs(1+\epsilon\sqrt{r}\mathrm{e}^{+\varphi})}, \quad \epsilon = \pm 1, \\ u_2(s,t,\varphi) &= \pm\sqrt{gt(1+\epsilon\sqrt{r}\mathrm{e}^{-\varphi})}. \end{aligned} \tag{3.4}$$

For fixed g, r this parameterization maps out a surface in (h,u) space by taking $s \geqslant 0$, $t \geqslant 0$ and $\varphi \in \mathbb{R}$ (when $\epsilon = +1$) and $\sqrt{r} \leqslant \mathrm{e}^{\varphi} \leqslant \frac{1}{\sqrt{r}}$ (when $\epsilon = -1$). Taking $\epsilon = +1$ gives the surface of criticality associated with the fast mode in Fig. 7 and $\epsilon = -1$ is associated with the slow mode. There does not appear to be an easy way to visualize this three-dimensional manifold.

4. The second derivative of P(c) on the criticality surface

As noted in the introduction, the second derivative of $\mathbf{P}(\mathbf{c})$ is of interest for the bifurcation analysis of solitary waves. The second derivative is also associated with singularities of the 3-manifold (3.4). The image of the criticality surface in (R_1, R_2, Q_1, Q_2) space can have singularities. In lower dimension these singularities show up as cuspoidal curves (cf. [10]). In higher dimension these singular sub-surfaces can still be found theoretically [2,7].

Define

$$\begin{aligned} f(\mathbf{c}) &:= \det\big[\mathrm{D}\mathbf{P}(\mathbf{c})\big] \\ &= \rho_1^2\rho_2^2\big[u_1^2u_2^2 - gh_2u_1^2 - gh_1u_2^2 + (1-r)g^2h_1h_2\big]. \end{aligned}$$

Then the criticality surface in (h_1, h_2, u_1, u_2) space is defined by $f^{-1}(0)$ and ∇f can be interpreted as a normal vector to the criticality surface. This vector is to be contrasted with $\mathbf{n}$ which is a normal vector to the image of $\mathbf{P}(\mathbf{c})$ when $\mathbf{c} \in f^{-1}(0)$.

A singularity occurs when the eigenvector $\mathbf{n}$ is tangent to the criticality surface, that is, $\nabla f \cdot \mathbf{n} = 0$. Now,

$$\nabla f = \rho_1^2\rho_2^2 \begin{pmatrix} -gu_2^2 + (1-r)g^2h_2 \\ -gu_1^2 + (1-r)g^2h_1 \\ 2u_1u_2^2 - 2gh_2u_1 \\ 2u_2u_1^2 - 2gh_2u_2 \end{pmatrix}.$$

Taking the inner product with $\mathbf{n}$ in (3.3),

$$\nabla f \cdot \mathbf{n} = -3gh_1h_2\frac{\rho_1^2\rho_2^2}{ab}\left\{\frac{u_1^2}{h_1^2}a^3 + r\frac{u_2^2}{h_2^2}b^3\right\}, \tag{4.1}$$

where a is an arbitrary nonzero constant and

$$b = \frac{1}{r}\left(\frac{u_1^2}{gh_1} - 1\right)a.$$

The function $\nabla f \cdot \mathbf{n}$ is related to the second derivative in (1.5) and (1.8) by

$$\nabla f \cdot \mathbf{n} = -\left(gh_1h_2\frac{\rho_1\rho_2^2}{ab}\right)\frac{d^2}{ds^2}\left(\mathbf{n}^T\mathbf{P}(\mathbf{c}+s\mathbf{n})\right)\Big|_{s=0}.$$

This identity can be verified by direct calculation, but it is a special case of a general result [7] for mappings from $\mathbb{R}^n$ to $\mathbb{R}^n$.

To simplify the expression (4.1) further, evaluate it on the (slow mode) criticality curve. The criticality condition (2.5) can be written in the form

$$\ell V(\ell)^4 - (m+\ell)V(\ell)^2 + m(1-r) = 0, \tag{4.2}$$

where m, ℓ are defined in (1.6) and

$$V(\ell)^2 := \frac{u_1^2}{gh_1}.$$

Solving (4.2) for $V(\ell)^2$ on the slow mode critical curve,

$$V(\ell)^2 = \frac{m+\ell-\sqrt{\delta}}{2\ell}, \quad \delta := (m+\ell)^2 - 4m\ell(1-r). \tag{4.3}$$

The velocity $V(\ell)^2$ is a generalization of V_0^2 in [16] and C_-^2 in [12] to include a velocity difference; specifically $C_-^2 = V_0^2 = V(1)^2$. Substitution in (4.1) gives

$$\frac{d^2}{ds^2}\left(\mathbf{n}^T\mathbf{P}(\mathbf{c}+s\mathbf{n})\right)\Big|_{s=0} = 3\rho_1V(\ell)^2\frac{g}{h_1}\frac{b^3}{m^3}\left(r\ell m - \left(m-\ell V(\ell)^2\right)^3\right).$$

Expanding and simplifying the right-hand side then leads to the fundamental formula

$$\frac{d^2}{ds^2}\left(\mathbf{n}^T\mathbf{P}(\mathbf{c}+s\mathbf{n})\right)\Big|_{s=0} = \mathsf{C}(\mathbf{c})\Phi(r,m,\ell), \tag{4.4}$$

with

$$\Phi(r,m,\ell) = m^2\ell^2r^2 + m\ell(3m-3\ell-1)r + (m-\ell)^3, \tag{4.5}$$

and

$$\mathsf{C}(\mathbf{c}) = -6g\rho_2\ell h_1b^3V(\ell)^2\big[h_2^2\big(2r\ell m - (m-\ell)^3 - 3m\ell r(m-\ell) + \sqrt{\delta}\big(m\ell r + (m-\ell)^2\big)\big)\big]^{-1}. \tag{4.6}$$

The zero set of the second derivative is determined by the function $\Phi(r,m,\ell)$. Before proceeding to analyze this function further, we show that this is a new interpretation of a well-known coefficient in the literature.

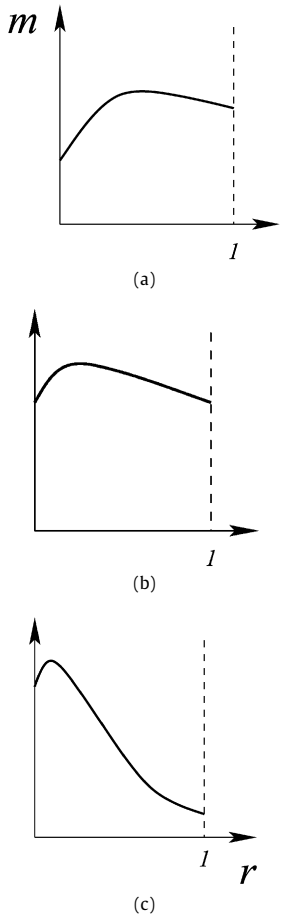

Fig. 8. Zero set of the function $\Phi(r,m,\ell)$ for the cases (a) $\ell < 1$, (b) $\ell = 1$ and (c) $\ell > 1$.

4.1. Comparison with Λ in Dias and Il'ichev [12]

The critical coefficient in Dias and Il'ichev [12] is Λ in Eq. (3.5) of [12]. It is the coefficient of the quadratic nonlinearity in the leading order normal form (Eq. (3.5) in [12]). In this subsection, the connection between Λ and the function $\Phi(r,m,\ell)$ with $\ell = 1$ is established.

The expression for Λ in [12] is

$$\Lambda = \frac{9(1-R)}{2C_-}\frac{\hat{\Lambda}}{C_-^2(1+H^2+3RH) - H(1+H)},$$

with

$$\hat{\Lambda} = C_-^4 + C_-^2(1-2H) + H^2 - 1. \tag{4.7}$$

Their notation corresponds to

$$H = \frac{h_2}{h_1} \quad \text{and} \quad R = \frac{\rho_2}{\rho_1},$$

and (Eq. (2.4) in [12])

$$C_-^2 = \frac{1+H-\sqrt{(1+H)^2 - 4H(1-R)}}{2}. \tag{4.8}$$

Substituting (4.8) into (4.7) and some rearrangement leads to

$$\hat{\Lambda} = \frac{\Phi(R,H,1)}{1+HR-(2-H)C_-^2}. \tag{4.9}$$

Hence $\Lambda = 0$ corresponds to $\Phi(R,H,1) = 0$. This curve is the dashed line plotted in Fig. 7 of [12] and it corresponds to the middle plot in Fig. 8.

Dias and Il'ichev also derive the critical coefficient another way. It is Eq. (A.22) in [12] and this equation can also be expressed in terms of Φ. Eq. (A.22) is

$$(\text{A.22}) = H_1(H_1-1)^2R^2 + H_1R\big(3-10H_1+7H_1^2\big) + \big(1-6H_1+12H_1^2-8H_1^3\big),$$

where

$$H_1 = \frac{h_1}{h_1+h_2} = \frac{1}{1+H}.$$

After some rearrangement we find

$$(\text{A.22}) = H_1^3\Phi(R,H,1).$$

This shows how Λ, (A.22) and $\Phi(r,m,1)$ are related.

4.2. Comparison with α_- in Kakutani and Yamasaki [16]

The critical coefficient in Kakutani and Yamasaki [16] is α_- in Eq. (3.8) of [16]. It is the coefficient of the nonlinear term in the KdV equation that they derive shown in Eq. (3.7) of their paper. Although the KdV equation derived there misses the generalized solitary waves, the critical coefficient is still the same as that in [12] and can be related to Φ.

In the notation of [16], the expression for the critical coefficient is

$$\alpha_- = \frac{3V_0^-\hat{\alpha}_-}{2((V_0^-)^2-m)\{(1+m)(V_0^-)^2-2(1-\sigma)m\}},$$

with

$$\hat{\alpha}_- = (1+m\sigma)\big(V_0^-\big)^2 - (1-\sigma)m(2-m).$$

In their notation $\sigma = \frac{\rho_2}{\rho_1}$ and (Eq. (2.12) in [16])

$$\big(V_0^-\big)^2 = \frac{1+m-\sqrt{(1+m)^2-4(1-\sigma)m}}{2}.$$

With a little manipulation it can be shown that

$$\alpha_- = \frac{2m(1-\sigma)\Phi(\sigma,m,1)}{\text{Den}},$$

where

$$\text{Den} = (1+m\sigma)(1+m) - 2m(2-m)(1-\sigma) - (1+m\sigma)\sqrt{(1+m)^2-4m(1-\sigma)}.$$

Therefore $\alpha_- = 0$ corresponds to $\Phi(\sigma,m,1)=0$, and the curve $\alpha_-=0$ is plotted in Fig. 2 of [16]. This case corresponds to the middle figure in Fig. 8.

5. Properties of $\Phi(r,m,\ell)$

The zeros of $\Phi(r,m,\ell)$ are important for the bifurcation of solitary waves and generalized solitary waves. $\Phi=0$ can signal the switch from a solitary wave of elevation to a solitary wave of depression, and it changes the nonlinearity from quadratic to cubic and so it is possible for fronts and generalized fronts to bifurcate at this point. In this section the zeros of $\Phi(r,m,\ell)$ are explored with emphasis on the implication of $\ell\neq 1$.

The function Φ is factorizable and so the zeros of Φ can be parametrized by

$$r = \frac{1+3\ell-3m}{2m\ell} \pm \frac{(1+\ell-m)\sqrt{1+4\ell-4m}}{2m\ell}. \tag{5.1}$$

This pair of curves is plotted in Fig. 8 for three ranges of velocity difference: $\ell<1$, $\ell=1$ and $\ell>1$. The case $\ell=1$, Fig. 8(b), recovers the result in [12,16] and Fig. 3 of Walker [21]. An important constraint on this curve is that $m\geqslant 1$ for all points satisfying $\Phi=0$, and so a necessary condition for $\Phi=0$ when $\ell=1$ is that the upper fluid depth be strictly greater than the lower fluid depth.

When $\ell\neq 1$ it is possible to have $h_2<h_1$ on the curve $\Phi=0$. For example, in the limits $r=0$ and $r=1$ we have

$$\Phi(0,m,\ell) = (m-\ell)^3 \quad\Rightarrow\quad m=\ell,$$
$$\Phi(1,m,\ell) = \big(m+\ell^2\big)\big(m^2-\ell\big) \quad\Rightarrow\quad m=\sqrt{\ell}.$$

Since ℓ can take any positive value, all depth ratios can occur on the $\Phi=0$ curve. A schematic of the case $\ell<1$ is shown in Fig. 8(a) and a schematic of the case $\ell>1$ is shown in Fig. 8(c).

The maximum value of m on the curve $\Phi=0$ is also of interest. The maximum of m occurs when $r^+=r^-$ in (5.1) which gives

$$m = 1+\ell \quad\text{or}\quad m=\frac{1+4\ell}{4},$$

and

$$r^{\max} = \frac{1+3\ell-3m}{2m\ell} \quad\text{with the constraint } m<\frac{1}{3}+\ell. \tag{5.2}$$

The root $m=1+\ell$ is nonphysical (since $r^{\max}$ in (5.2) is negative in this case). Therefore the value of m when $r=r^{\max}$ is

$$m^{\max} = \frac{1+4\ell}{4}.$$

When $\ell=1$, $m^{\max}$ reduces to the familiar value of $\frac{5}{4}$ [16]. For arbitrary positive ℓ, substitution of $m^{\max}$ into (5.2) gives

$$r^{\max} = \frac{1}{2\ell(1+4\ell)}.$$

In terms of dimensional coordinates this is

$$\left(\frac{\rho_2}{\rho_1}\right)^{\max} = \frac{1}{2\ell(1+4\ell)} \quad\text{and}\quad \left(\frac{h_2}{h_1}\right)^{\max} = \frac{1+4\ell}{4},$$

where

$$\ell = \frac{u_2^2}{u_1^2}, \quad \frac{1}{4}\leqslant \ell < +\infty$$

and

$$V(\ell)^2\big|_{\max} = \left(\frac{u_1^2}{gh_1}\right)^{\max} = \frac{4\ell-1}{4\ell}.$$

Note that $V(\ell)\to 0$ as $\ell\to\frac{1}{4}^+$. With ℓ varying, a much wider range of critical density ratios can be achieved, whereas with $\ell=1$ we only have the value $r^{\max}=\frac{1}{10}$.

One implication of a nonzero velocity difference is that there is a potential for Kelvin–Helmholtz instability [6]. Without surface tension, all flows with nonzero velocity difference are unstable, and with surface tension there is a critical value of the velocity difference below which the uniform flow is stable. The role of Kelvin–Helmholtz instability will not be considered in this paper, as it requires bringing in time dependence. However, it is of interest to look at the velocity difference on the surface of criticality. Using the parameterization (3.4) the velocity difference on the surface of criticality (the slow mode) is

$$\frac{u_2^2-u_1^2}{gh_1} = m-1+\sqrt{r}\,\mathrm{e}^{\varphi} - m\sqrt{r}\,\mathrm{e}^{-\varphi}, \quad \sqrt{r}<\mathrm{e}^{\varphi}<\frac{1}{\sqrt{r}}.$$

Hence the velocity difference varies over the criticality surface, and there is a distinguished curve on the criticality surface where the velocity difference vanishes:

$$\sqrt{r}z^2+(m-1)z-m\sqrt{r}=0, \quad z=\mathrm{e}^{\varphi}.$$

This quadratic has one positive root for each (r, m) given by

$$e^{\varphi} = \frac{\sqrt{(m-1)^2 + 4mr} + 1 - m}{2\sqrt{r}}.$$

Hence, there is a subset of the criticality surface where Kelvin–Helmholtz instability can be avoided completely. But there are also regions where the Kelvin–Helmholtz instability is operative, and so there will be dynamical implications.

6. The role of criticality in the generation of solitary waves

Criticality is a property of the nonlinearity and it occurs in the shallow water equations or the full equations. However, in order to generate solitary waves out of criticality a balance between nonlinearity and dispersion is needed. In the full equations, this dispersion is implicit. Here, the shallow water equations will be used for illustration. Adding the simplest form of dispersion to the shallow water model (1.1) leads to

$$\begin{aligned}
&\frac{\partial}{\partial t}(\rho_1 h_1) + \frac{\partial}{\partial x}(\rho_1 h_1 u_1) = 0,\\
&\frac{\partial}{\partial t}(\rho_2 h_2) + \frac{\partial}{\partial x}(\rho_2 h_2 u_2) = 0,\\
&\frac{\partial}{\partial t}(\rho_1 u_1) + \frac{\partial}{\partial x}\left(\frac{1}{2}\rho_1 u_1^2 + \rho_1 g h_1 + \rho_2 g h_2\right) = a_{11}\frac{\partial^3 h_1}{\partial x^3} + a_{12}\frac{\partial^3 h_2}{\partial x^3},\\
&\frac{\partial}{\partial t}(\rho_2 u_2) + \frac{\partial}{\partial x}\left(\frac{1}{2}\rho_2 u_2^2 + \rho_2 g h_1 + \rho_2 g h_2\right) = a_{21}\frac{\partial^3 h_1}{\partial x^3} + a_{22}\frac{\partial^3 h_2}{\partial x^3}.
\end{aligned} \tag{6.1}$$

Explicit expressions for the coefficients can be obtained using a Boussinesq approximation (see Chapter 2 of Donaldson [13]), but will not be needed here except for the symmetry property $a_{21} = a_{12}$. There are many other variants of the leading order Boussinesq model for two layer flow (e.g. [5,11]), but the form (6.1) will be sufficient for the present purposes.

The steady equations reduce to

$$\begin{aligned}
&\rho_1 h_1 u_1 = q_1, \quad \frac{dq_1}{dx} = 0,\\
&\rho_2 h_2 u_2 = q_2, \quad \frac{dq_2}{dx} = 0,\\
&\frac{1}{2}\rho_1 u_1^2 + \rho_1 g h_1 + \rho_2 g h_2 = \frac{dH_1}{dx} + r_1, \quad \frac{dr_1}{dx} = 0,\\
&\frac{1}{2}\rho_2 u_2^2 + \rho_2 g h_1 + \rho_2 g h_2 = \frac{dH_2}{dx} + r_2, \quad \frac{dr_2}{dx} = 0,\\
&a_{11}\frac{dh_1}{dx} + a_{12}\frac{dh_2}{dx} = H_1,\\
&a_{21}\frac{dh_1}{dx} + a_{22}\frac{dh_2}{dx} = H_2.
\end{aligned}$$

This system can be characterized as a Hamiltonian system with dimension twelve in a way that highlights the role of criticality of uniform flows in the generation of solitary waves. Introduce potentials

$$h_1 = \frac{d\gamma_1}{dx}, \quad h_2 = \frac{d\gamma_2}{dx}, \quad u_1 = \frac{d\phi_1}{dx}, \quad u_2 = \frac{d\phi_2}{dx},$$

and new coordinates

$$Z := (h_1, h_2, q_1, q_2, H_1, H_2, \phi_1, \phi_2, \gamma_1, \gamma_2, r_1, r_2). \tag{6.2}$$

Then the steady equations are equivalent to the Hamiltonian system

$$\mathbf{J}Z_x = \nabla S(Z), \quad Z \in \mathbb{R}^{12} \tag{6.3}$$

with Hamiltonian function

$$\begin{aligned}
S(Z) = {} & r_1 h_1 + r_2 h_2 - \frac{1}{2}\rho_1 g h_1^2 - \rho_2 g h_1 h_2 - \frac{1}{2}\rho_2 h_2^2\\
& + \frac{1}{2}\frac{q_1^2}{\rho_1 h_1} + \frac{1}{2}\frac{q_2^2}{\rho_2 h_2} + \frac{1}{2}\frac{a_{22}}{D}H_1^2 - \frac{a_{12}}{D}H_1 H_2 + \frac{1}{2}\frac{a_{11}}{D}H_2^2,
\end{aligned}$$

where $D = a_{11}a_{22} - a_{12}^2$ and symplectic operator

$$\mathbf{J} = \begin{bmatrix}
0 & 0 & 0 & 0 & -1 & 0 & 0 & 0 & 0 & 0 & 0 & 0\\
0 & 0 & 0 & 0 & 0 & -1 & 0 & 0 & 0 & 0 & 0 & 0\\
0 & 0 & 0 & 0 & 0 & 0 & 1 & 0 & 0 & 0 & 0 & 0\\
0 & 0 & 0 & 0 & 0 & 0 & 0 & 1 & 0 & 0 & 0 & 0\\
1 & 0 & 0 & 0 & 0 & 0 & 0 & 0 & 0 & 0 & 0 & 0\\
0 & 1 & 0 & 0 & 0 & 0 & 0 & 0 & 0 & 0 & 0 & 0\\
0 & 0 & -1 & 0 & 0 & 0 & 0 & 0 & 0 & 0 & 0 & 0\\
0 & 0 & 0 & -1 & 0 & 0 & 0 & 0 & 0 & 0 & 0 & 0\\
0 & 0 & 0 & 0 & 0 & 0 & 0 & 0 & 0 & 0 & -1 & 0\\
0 & 0 & 0 & 0 & 0 & 0 & 0 & 0 & 0 & 0 & 0 & -1\\
0 & 0 & 0 & 0 & 0 & 0 & 0 & 0 & 1 & 0 & 0 & 0\\
0 & 0 & 0 & 0 & 0 & 0 & 0 & 0 & 0 & 1 & 0 & 0
\end{bmatrix}.$$

6.1. Weakly nonlinear normal form for bifurcating solitary waves

Here, the weakly nonlinear bifurcation of solitary waves from the uniform flow will be sketched with an emphasis on how the normal form theory of [12] is modified by (a) the Hamiltonian structure and (b) the inclusion of the full four-parameter family of uniform flows.

The Hamiltonian system (6.3) has dimension 12 but 8 of these dimensions are associated with the uniform flow. By inspection, it is clear that one can reduce to a Hamiltonian system on $\mathbb{R}^4$ with coordinates (h_1, h_2, H_1, H_2). However, by maintaining the additional terms the system includes a geometric formulation of uniform flows.

The system (6.3) has a 4-dimensional symmetry group. This symmetry is simple (one can add an arbitrary constant to γ_1, γ_2, ϕ_1 and ϕ_2) but relative equilibria (RE) associated with this symmetry are uniform flows. These RE are degenerate precisely when the uniform flows are critical.

Given a 4-parameter family of RE of (6.3) at criticality the strategy is to perturb (6.3) about this family and then use normal form theory to get the weakly nonlinear system near the RE. By combining the normal form for degenerate RE [7–9] and the normal form for a double zero eigenvalue with a pair of purely imaginary eigenvalues in [12], the weakly nonlinear normal form is

$$\begin{aligned}
&-\frac{dI_j}{dx} = 0, \quad j = 1, \ldots, 4,\\
&-\frac{dv}{dx} = I_1 - \frac{1}{2}\kappa u^2 + \nu|A|^2 + \cdots,\\
&\frac{d\psi_1}{dx} = u + \cdots,\\
&\frac{d\psi_j}{dx} = s_j I_j + \cdots, \quad j = 2, 3, 4,\\
&\frac{du}{dx} = s_1 v + \cdots,\\
&\frac{dA}{dx} = \mathrm{i}\omega A + \mathrm{i}\nu u A + \cdots.
\end{aligned} \tag{6.4}$$

The first four equations $\frac{dI_j}{dx} = 0$ just state that solutions stay on surfaces of constant mass flux and Bernoulli energy. The phases ψ_j are the dual Hamiltonian variables to the I_j and they represent perturbations of the potentials γ_1, γ_2 and ϕ_1, ϕ_2. Reducing, by eliminating (I_j, ψ_j), $j = 1, \ldots, 4$, recovers the normal form of Dias and Il'ichev with the Hamiltonian constraint that the coefficient of $|A|^2$ in the v_x equation should be the same as the coefficient

of iuA in the A_x equation. The parameters $s_j = \pm 1$ are symplectic signs and their role is discussed in [7]. Our main observation, as noted in Eq. (1.5) in the introduction, is that κ is determined by the second derivative of the mapping $\mathbf{P}(\mathbf{c})$.

Eliminating the symmetry variables, the normal form reduces to

$$-s_1\frac{d^2u}{dx^2} = I_1 - \frac{1}{2}\kappa u^2 + \nu|A|^2 + \cdots,$$
$$\frac{dA}{dx} = i\omega A + i\nu uA + \cdots \tag{6.5}$$

with $s_1 = \pm 1$, I_1 is a measure of the distance from the criticality surface, κ is given by (1.5) and ν and ω are given in [12]. Neglecting the higher order terms this system is integrable and explicit expressions can be written down for the solitary waves and generalized solitary waves. Clearly $|A(x)|^2$ is constant, and so the first equation in (6.5) has a solution which is a constant plus a sech^2 solitary wave. The nonclassical nature of the solitary wave is due to $|A(x)| \neq 0$. A detailed analysis of the various forms of these solitary waves is given in [12]. The only difference here is the extended range of parameter space, and with the extended normal form (6.4), the coupling with the mean flow (uniform flow) can be made explicit.

7. Concluding remarks

In this paper we have concentrated on criticality of uniform flows. However, as shown in [9], criticality also applies to the periodic travelling waves bifurcating from the uniform flows (in the case of one layer, these periodic travelling waves are the Stokes wave in shallow water). Criticality of the periodic state coupled to a mean flow is called secondary criticality in [9]. This form of criticality leads to a secondary bifurcation of steady dark solitary waves (generalizing the bifurcation of classical solitary waves when uniform flows are critical). For the case of two layers with an upper free surface these waves will be more exotic since there is the potential for generalized tails. Application of the theory in [9] shows that one should add B, the wave action flux, to the set of functionals (R_1, R_2, Q_1, Q_2). In addition to (h_1, h_2, u_1, u_2) one includes k the wavenumber of the periodic wave at the interface. Then one can show that *the coupled system is critical* when the determinant of the extended 5×5 Jacobian matrix vanishes,

$$\det\left[\frac{\partial(R_1, R_2, Q_1, Q_2, B)}{\partial(h_1, h_2, u_1, u_2, k)}\right] = 0.$$

When this condition is satisfied for periodic waves at the interface between two fluids with a free surface coupled to a 4-component mean flow – and there is good reason to suspect that it is satisfied for some parameter values – application of the theory in [9] would lead to the secondary bifurcation of a new kind of dark solitary wave at the interface.

Acknowledgements

The authors are grateful to an anonymous referee for helpful comments, particularly the suggestion to prove that $\Delta'(0)$ is nonzero, which is now included as an appendix. The work of Neil Donaldson was supported by a PhD studentship awarded by EPSRC.

Appendix A. Proof that DP(c) has rank 3 at criticality

To prove that $\Delta'(0) \neq 0$, first rearrange $\Delta'(0)$ in (3.2) into the form

$$\Delta'(0) = r\rho_1^3\big[rgh_2(g+h_1)\big[(1-r)F_2^2 - 1\big] + gh_1(g+h_2)\big[(1-r)F_1^2 - 1\big] + rg^2(h_1 + rh_2)\big]. \tag{A.1}$$

Use the criticality condition in the form (2.5) to eliminate F_2^2,

$$\Delta'(0) = \frac{r\rho_1^3}{[(1-r)F_1^2 - 1]}\big[r^2gh_2(g+h_1) + gh_1(g+h_2)\big[(1-r)F_1^2 - 1\big]^2 + rg^2(h_1 + rh_2)\big[(1-r)F_1^2 - 1\big]\big],$$

or

$$\Delta'(0) = \frac{r\rho_1^3}{[(1-r)F_1^2 - 1]}\big[gh_2B^2 + g^2h_1(1-r)\big[(1-r)F_1^2 - 1\big]\big(F_1^2 - 1\big)\big], \tag{A.2}$$

with

$$B^2 = r^2h_1 + h_1\big[(1-r)F_1^2 - 1\big]^2 + r^2g(1-r)F_1^2.$$

The term B^2 is strictly positive along both the slow and fast criticality curves. The key term is the product

$$\big[(1-r)F_1^2 - 1\big]\big(F_1^2 - 1\big), \tag{A.3}$$

in the second term in the right-hand side of (A.2). However, along the fast criticality curve $(1-r)F_1^2 - 1$ and $F_1^2 - 1$ are positive. Hence, $\Delta'(0)$ is strictly positive along the fast criticality curve.

Along the slow criticality curve $(1-r)F_1^2 - 1 < 0$ but $F_1^2 \leqslant 1$, the latter inequality following from Fig. 7, or from the parameterization of (2.5). Hence the product (A.3) is either positive or zero. When it is zero, the argument in (A.2) is still positive since $B^2 > 0$. Hence, $\Delta'(0)$ is strictly negative along the slow criticality curve. This completes the proof that $D\mathbf{P}(\mathbf{c})$ has rank 3 at all parameter values that are physically relevant (i.e. $h_1 > 0$, $h_2 > 0$, $g > 0$ and $0 < r < 1$).

References

[1] L. Armi, The hydraulics of two flowing layers with different densities, J. Fluid Mech. 163 (1986) 27–58.
[2] V.I. Arnold, S.M. Gusein-Zade, A.N. Varchenko, Singularities of Differentiable Maps, vol. I, Birkhäuser, Boston, 1985.
[3] P.G. Baines, Topographic Effects in Stratified Flows, Cambridge University Press, 1995.
[4] R. Barros, Conservation laws for one-dimensional shallow-water models for one and two-layer flows, Math. Models Methods Appl. Sci. 16 (2006) 119–137.
[5] R. Barros, S.L. Gavrilyuk, Dispersive nonlinear waves in two-layer flows with free surface. Part II: Large amplitude solitary waves embedded into the continuous spectrum, Stud. Appl. Math. 119 (2007) 213–251.
[6] T.B. Benjamin, T.J. Bridges, Reappraisal of the Kelvin–Helmholtz instability. Part 1. Hamiltonian structure, J. Fluid Mech. 333 (1997) 301–325.
[7] T.J. Bridges, Degenerate relative equilibria, curvature of the momentum map, and homoclinic bifurcation, J. Differential Equations 244 (2008) 1629–1674.
[8] T.J. Bridges, N.M. Donaldson, Degenerate periodic orbits and homoclinic torus bifurcation, Phys. Rev. Lett. 95 (10) (2005) 104301.
[9] T.J. Bridges, N.M. Donaldson, Secondary criticality of water waves. Part 1. Definition, bifurcation and solitary waves, J. Fluid Mech. 565 (2006) 381–417.
[10] T.J. Bridges, N.M. Donaldson, Reappraisal of criticality for two-layer flows and its role in the generation of internal solitary waves, Phys. Fluids 19 (2007) 072111.
[11] W. Craig, P. Guyenne, H. Kalisch, Hamiltonian long-wave expansions for free surfaces and interfaces, Comm. Pure Appl. Math. 58 (2005) 1587–1641.
[12] F. Dias, A. Il'ichev, Interfacial waves with free-surface boundary conditions: an approach via a model equation, Physica D 150 (2001) 278–300.
[13] N.M. Donaldson, Criticality theory and conformal mapping techniques for single and two-layer water-wave systems, PhD Thesis, University of Surrey, 2006.
[14] R.H.J. Grimshaw, Internal solitary waves, in: Adv. in Fluid Mech. V, in: Adv. Fluid Mech., vol. 40, WIT Press, Southampton, 2004, pp. 209–218.
[15] K.R. Helfrich, W.K. Melville, Long nonlinear internal waves, Annu. Rev. Fluid Mech. 38 (2006) 395–425.
[16] T. Kakutani, N. Yamasaki, Solitary waves on a two-layer fluid, J. Phys. Soc. Japan 45 (1978) 674–679.
[17] E. Lombardi, Oscillatory Integrals and Phenomena Beyond All Algebraic Orders, Lecture Notes in Math., vol. 1741, Springer, Berlin, 2000.

[18] H. Michallet, F. Dias, Numerical study of generalized interfacial solitary waves, Physics of Fluids 11 (1999) 1502–1511.
[19] A.S. Peters, J.J. Stoker, Solitary waves in liquids having non-constant density, Comm. Pure Appl. Math. 13 (1960) 115–164.
[20] M.J. Sewell, D. Porter, Constitutive surfaces in fluid mechanics, Math. Proc. Cambridge Philos. Soc. 88 (1980) 517–546.
[21] L.R. Walker, Interfacial solitary waves in a two-fluid medium, Phys. Fluids 16 (1973) 1796–1804.